Acta Cryst. (1954). 7, 801

The Crystal Structure of Potassium Metavanadate Monohydrate, $KVO_3.H_2O$*

By C. L. Christ, Joan R. Clark and H. T. Evans, Jr.

U.S. Geological Survey, Washington 25, D.C., U.S.A.

(*Received* 11 *May* 1954)

$KVO_3.H_2O$ is orthorhombic, *Pnam*, $a = 8{\cdot}15_1$, $b = 13{\cdot}58_6$, $c = 3{\cdot}69_7$ Å, $Z = 4$. A trial structure, established by the use of a vector-shift method applied to the Patterson projection on (001), was refined by electron-density projections (including bounded projections) and by least-squares analysis. In the structure each vanadium atom is linked to five oxygen atoms to form a distorted trigonal dipyramid; the polyhedra so formed share edges to form continuous chains parallel to the *c* axis. This fivefold coordination is analogous to that which exists in V_2O_5.

Introduction

When vanadium pentoxide is dissolved in a solution of potassium hydroxide, and the solution is maintained at a pH between 6·5 and 8, clear colorless needles of both potassium metavanadate, KVO_3, and its monohydrate, $KVO_3.H_2O$, are readily produced on concentration and cooling. This pH range comprises the so-called 'metavanadate' stability range, in contrast with the range of pH > 10 corresponding to the 'orthovanadates', the range from pH 8 to 10 corresponding to the 'pyrovanadates', and the range corresponding to the orange 'polyvanadates' from pH 6·5 to the isoelectric point at pH 1·6, at which point brown V_2O_5 hydrates precipitate. The system Na_2O–V_2O_5–H_2O, which is characterized in a general way by the stability ranges referred to, has been the subject of considerable study of various workers and by various physical chemical methods [see for example Düllberg (1903), Jander & Jahr (1933), Souchay & Carpeni (1946), Ducret (1951)]. Although the reactions involved are usually considered to be a series of successive condensations toward higher molecular weight complexes with increasing acidity, no details have been established to date concerning any of the molecular structures, or any of the mechanisms involved. In the U.S. Geological Survey laboratories we are making an attempt to approach the problem of the constitution and interrelation of the many phases present in the system K_2O–V_2O_5–H_2O by means of crystal-structure analysis of the solids that appear. In this paper the crystal structure of $KVO_3.H_2O$ is described in detail [a preliminary account has been given in Christ, Clark & Evans (1953)]. A study of the structure of KVO_3 has been completed and will be described in a forthcoming article.

KVO_3 and $KVO_3.H_2O$, although their crystal structures have been revealed to be entirely different, are similar in chemical and physical properties and mode of genesis. Both are sparingly soluble in cold water and readily soluble in hot water, and both have pronounced fibrous cleavage. When a potassium metavanadate solution is rapidly cooled, a crystalline precipitate characterized by fine hairlike needles appears, which is mainly KVO_3. As the rate of cooling slows at lower temperatures, needles of similar habit of $KVO_3.H_2O$ are also formed. On very slow crystallization by evaporation, radiating groups of blunt rods of $KVO_3.H_2O$ are produced, sometimes simultaneously and in contact with stubby, pseudo-octahedral crystals of KVO_3. $KVO_3.H_2O$ apparently converts to KVO_3 on grinding.

$KVO_3.H_2O$ was first recognized by Norblad (1875) and was noted by Fock (1889), but otherwise to our knowledge it is not mentioned in the literature.

Experimental work

Preparation of crystals and chemical analysis

At the beginning of this investigation it was believed that the two compounds crystallizing in the pH range between 6·5 and 8 were polymorphic forms of KVO_3. The structure analysis, however, soon showed clearly that the substance dealt with here was a monohydrate and was entirely consistent with a compound of formula $KVO_3.H_2O$. With this in mind it was then possible to resolve the difficulties in chemical analysis that arose from dealing with a mixture. By very slow crystallization, mixtures were prepared containing crystals sufficiently large to ensure efficient separation. An analysis of the $KVO_3.H_2O$ obtained in this way is given below:

	Found (%)	Theoretical (%)
K_2O	30·24	30·18
V_2O_5	58·40	58·28
H_2O	11·64	11·54
Total	100·28	100·00

(Analyst, George B. Magin, Jr., U.S. Geological Survey.)

The typical blunt-rod habit of $KVO_3.H_2O$ is shown in Fig. 1.

* Publication authorized by the Director, U.S. Geological Survey.

Space group and unit-cell dimensions

Zero- and upper-level photographs around [001], made on both Weissenberg and precession cameras and

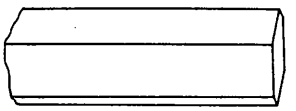

Fig. 1. Typical blunt-rod crystal of $KVO_3.H_2O$.

with both zirconium-filtered Mo $K\alpha$(Mo/Zr) and nickel-filtered Cu $K\alpha$(Cu/Ni) radiations, were used to establish the lattice type and symmetry. Systematic extinctions were found to be of the type $h0l$, $h \neq 2n$, and $0kl$, $k+l \neq 2n$. These lead to the space groups $Pnam$–D_{2h}^{16} or Pna–C_{2v}^{9}. Visual examination of the reflections obtained on rotation patterns made around [001] establishes that corresponding reflections on all even-layer lines are similar, as are those on all odd-layer lines. It follows that in this structure most atoms are situated on planes parallel to (001) and $\frac{1}{2}c$ apart. This fact suggests that all the atoms lie on mirror planes in the space group $Pnam$, and on this assumption a satisfactory structure has been determined.

Table 1. *X-ray powder data for* $KVO_3.H_2O$ *and* KVO_3

These data correspond to a mixture of $KVO_3.H_2O$ and KVO_3 that is obtained when crystals of $KVO_3.H_2O$ are powdered. The d_{hkl} values for $KVO_3.H_2O$ are calculated from the lattice constants given in the text; the d_{hkl} values for KVO_3 are derived from the following data: orthorhombic $a = 5{\cdot}70$, $b = 10{\cdot}82$, $c = 5{\cdot}22$ Å. The lines were indexed with the help of a KVO_3 powder pattern. Cu/Ni radiation $\lambda = 1{\cdot}5418$ Å was used. Data are listed only for $d_{hkl} > 2{\cdot}00$ Å. The lines corresponding to KVO_3 are so indicated, the other lines being due to $KVO_3.H_2O$.

Measured		Calculated		
I	d_{hkl} (Å)	d_{hkl} (Å)	hkl	
15	7·00	6·99	110	
5	5·39	5·41	020	KVO_3
9	5·20	5·22	001	KVO_3
		5·22	120	
10	3·910	3·904	210	
		3·924	120	KVO_3
8	3·748	3·756	021	KVO_3
10	3·488	3·495	220	
7	3·262	3·268	111	
14	3·128	3·135	140	
		3·136	121	KVO_3
11	3·024	3·017	121	
		3·030	230	
13	2·854	2·850	200	KVO_3
		2·864	031	
4	2·735	2·738	201	
11	2·680	2·684	211	
		2·702	131	
8	2·607	2·609	240	
		2·610	002	KVO_3
7	2·526	2·521	220	KVO_3
		2·523	320	
8	2·440	2·437	211	KVO_3
5	2·402	2·402	041	KVO_3
7	2·342	2·343	231	
7	2·302	2·318	112	KVO_3
9	2·257	2·261	250	
		2·264	060	
4	2·179	2·182	160	
4	2·125	2·122	340	
3	2·043	2·038	400	

Lattice-constant measurements were made with a precession camera, the crystal-to-film distance of which had been accurately calibrated by use of a quartz crystal. Patterns of the ($h0l$) and ($0kl$) zones were prepared using Mo/Zr radiation and were corrected for horizontal and vertical shrinkage. The values of the cell edges derived from these patterns were checked against those derived from a powder pattern made with Cu/Ni radiation. The powder data are given in Table 1. As $KVO_3.H_2O$ converts to KVO_3 on grinding, it was impossible to prepare a powder pattern of $KVO_3.H_2O$ only; the data of Table 1 correspond to the mixture. The crystallographic data for $KVO_3.H_2O$ are given below:

Orthorhombic; space group: $Pnam$–D_{2h}^{16}.
$a = 8{\cdot}15_1 \pm 0{\cdot}008$, $b = 13{\cdot}58_6 \pm 0{\cdot}010$, $c = 3{\cdot}69_7 \pm 0{\cdot}004$ Å.

(Mo λ: $K\alpha = 0{\cdot}71069$ Å; $K\alpha_1 = 0{\cdot}70926$ Å).
Cell contents: $4(KVO_3.H_2O)$.
Density (calc.) = 2·53 g.cm.$^{-3}$, density (obs.) = 2·52 g.cm.$^{-3}$.

Intensity measurements

For the intensity measurements multiple-film Weissenberg patterns using Mo/Zr radiation were prepared. Three films interleaved with 0·0005 in. Ni foil were used for each exposure. The ($hk0$) and ($hk1$) zones were recorded from a prismatic crystal having nearly equidimensional cross section, approximately $0{\cdot}1 \times 0{\cdot}1$ mm. A comparison strip of intensities was prepared by recording a given reflection from the crystal for varying known lengths of time, using the same experimental set-up and crystal as were used in preparing the Weissenberg patterns. The estimated intensities were converted to $|F_{hkl}|^2$ values through the use of the Lorentz- and polarization-factor tables of Buerger & Klein (1945) for the $hk0$'s and the Lp chart of Cochran (1948) for the $hk1$'s. No attempt was made to correct for absorption effects, which were assumed to be relatively small owing to the small cross-sectional size of the crystal used and to use of Mo $K\alpha$ radiation.

Other considerations

In the initial stages of the analysis the observed and calculated structure factors were related by use of the scaling constant k, where $k\Sigma|F_o| = \Sigma|F_c|$. Subsequently the relation $k|F_o| = |F_c| \exp[-B(\sin^2\theta)/\lambda^2]$ was used to fix the absolute scale of the observed structure factors and the value of the coefficient B of the temperature factor. For the final values of the coordinates, $B = 1{\cdot}22$ Å^2 for the ($hk0$) zone and 0·71 Å^2 for the ($hk1$) zone.

The Hartree atomic scattering curve for O^{-2} was used for the oxygen atoms and for the water molecule. For K^+ a scattering curve corresponding to the

Thomas–Fermi values for K for $(\sin\theta)/\lambda \geq 0{\cdot}1$ Å^{-1} and smoothed in to $f = 18$ for $(\sin\theta)/\lambda = 0$ was used. At the beginning of the structural analysis a curve prepared in an analogous fashion for V^{+5} was used. It was later found that significant improvement in the agreement between calculated and observed structure factors at small $(\sin\theta)/\lambda$ values was obtained when the Thomas–Fermi values for V were used. The subsequent refinement was made using these values. All values of the scattering factors were taken from the *International Tables* (1935).

Maxima on the electron-density maps used in determining the structure were located by the method of Booth (1948).

Determination and refinement of the structure

The structural problem consists in determining the parameters of one V, one K, three O, and one H_2O in the positions 4(c) of the space group *Pnam* (*International Tables*, 1935). The relatively short c axis suggested the use of the Patterson projection on (001) for the determination of the essential features of this structure, and accordingly this projection was prepared with the $|F_{hk0}|^2$ values on an arbitrary basis and the $|F_{000}|^2$ term omitted. Buerger (1951) has shown how the Patterson projection on (001) for a crystal of similar symmetry and dimensions, berthierite, $FeSb_2S_4$ (*Pnam*, $a = 11{\cdot}44$, $b = 14{\cdot}12$, $c = 3{\cdot}76$ Å, $Z = 4$), may be converted to an approximate electron-density map through the use of his minimum-function analysis. Buerger's procedure for $FeSb_2S_4$ was followed for $KVO_3.H_2O$ and the approximate $\varrho_z(x, y)$ map shown in Fig. 2 was obtained.* From this map x and y

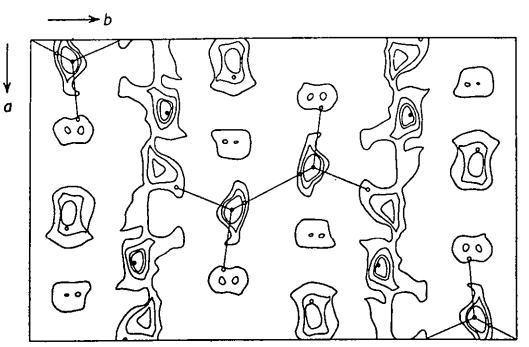

Fig. 2. Approximate $\varrho_z(x, y)$ map obtained by the minimum-function method. The final atomic positions are indicated by the small circles.

coordinates for the two heavy atoms K and V were assigned and structure factors F_{hk0} calculated using the same atomic scattering curve for both atoms, that of K^+. These coordinates are given in column (1) of

* With the $|F_{000}|^2$ term omitted it was necessary to contour all the levels of the Patterson map, including the negative ones, in order to finish with a meaningful approximate $\varrho_z(x, y)$ map.

Table 2. *Atomic positional parameters for* $KVO_3.H_2O$

	Parameters†	Stage of refinement* (1)	(2)	(3)	(4) (final)
V	x	0·07	0·073	0·074	0·074
	y	0·08	0·080	0·082	0·082
K	x	−0·23	−0·244	−0·244	−0·244
	y	−0·28	−0·279	−0·278	−0·278
O_I	x	—	−0·003	−0·005	−0·005
	y	—	0·198	0·195	0·192
O_{II}	x	—	0·267	0·276	0·277
	y	—	0·100	0·095	0·096
O_{III}	x	—	−0·058	−0·046	−0·041
	y	—	−0·042	−0·048	−0·047
H_2O	x	—	0·125	0·119	0·118
	y	—	0·420	0·414	0·412
R‡		0·45	0·316	0·159	0·142 ($hk0$)
				0·194	§ ($hk1$)

* See text for description of stage of refinement.
† All atoms in the asymmetric unit at $z = \frac{1}{4}$.
‡ Discrepancy factor.
§ Not calculated.

Table 2, which lists the coordinates and the discrepancy factor R found for each stage of the refinement. Signs calculated on the basis of these coordinates permitted the evaluation of $\varrho_z(x, y)$ using 87 terms. From this map, coordinates for all the atoms, but not for the water molecule, were assigned and a second $\varrho_z(x, y)$ containing 136 terms was calculated. Actually, a peak corresponding to the water molecule appeared on the first $\varrho_z(x, y)$ map as well as on the approximate $\varrho_z(x, y)$ map derived from the Patterson function. As it was believed that the compound was anhydrous, this peak was dismissed as being spurious and was expected to disappear in subsequent electron-density refinement, but at the completion of the second $\varrho_z(x, y)$ map, it was realized that the peak was real and that the compound was a monohydrate. This was fully verified, first, by the completed structural analysis and subsequently by chemical analysis, as explained previously. The coordinates assigned on the basis of the second $\varrho_z(x, y)$ map are given in Table 2, column (2). Two successive $\varrho_z(x, y)$ maps were then prepared, the second of which contained 152 F_{hk0}'s, on an absolute scale, corresponding to all of the non-zero intensities measured. Parameters derived from this last map were then used in fixing the signs of the F_{hkl}'s entering in a bounded electron-density projection described below.

All of the atoms are well resolved in the electron-density projection $\varrho_z(x, y)$ except V and O_{III}. To obtain parameters for these atoms and to check the parameters of the other atoms, the projection on (001) of the electron density between $z = 0$ and $z = \frac{1}{2}$ was prepared, following the method of Booth (1948). The expression for the bounded projection of interest here has the form

$$S(x,y) = \tfrac{1}{2}\left[\frac{1}{A}\sum_{h}^{-\infty}\sum_{k}^{\infty} F_{hk0}\cos 2\pi(hx+ky) - \frac{2}{\pi A}\sum_{h}\sum_{k}^{-\infty}\sum_{l}^{l=2n+1}\frac{F_{hkl}}{l}\sin 2\pi(hx+ky)\right]. \quad (1)$$

The first sum within the brackets of equation (1) is simply the usual electron-density projection on (001); hence the equation may be rewritten as

$$S(x,y) = \tfrac{1}{2}\left[\varrho_z(x,y) - \frac{2}{\pi A}S'(x,y)\right], \quad (2)$$

where

$$S'(x,y) = \sum_{h}\sum_{k}^{-\infty}\sum_{l}^{l=2n+1}\frac{F_{hkl}}{l}\sin 2\pi(hx+ky). \quad (3)$$

For the space group *Pnam*, equation (3) reduces to

$$\frac{S'(x,y)}{4} = \sum_{h}^{h+k=2n}\sum_{k}^{\infty} F'_{hk}\sin 2\pi hx\cos 2\pi ky + \sum_{h}^{h+k=2n+1}\sum_{k}^{\infty} F'_{hk}\cos 2\pi hx\sin 2\pi ky, \quad (4)$$

where

$$F'_{hk} = \sum_{l}^{-\infty}\frac{F_{hkl}}{l}.$$

In evaluating $S'(x,y)$ the F_{hkl} values for $l \neq 1$ ($l = 2n+1$) were derived from the F_{hk1} values in the following way: it was assumed that within a sufficient degree of approximation the shape of the scattering curves of the atoms involved is the same as that of some average reference atom. In the present case the reference scattering curve was taken as the average of the curves of K^+ and V because these atoms contribute much more than the O atoms to the scattering. If one writes the atomic scattering factor in the form

$$f_i(hkl) = Z_i g(hkl),$$

where $g(hkl)$ defines the shape of the reference scattering curve, then for *Pnam* and $z = \frac{1}{4}$ for the atoms of the asymmetric unit, it follows that

$$\frac{F_{hk1}}{g(hk1)} = -\frac{F_{hk3}}{g(hk3)} = \frac{F_{hk5}}{g(hk5)} = \ldots = (-1)^{\frac{n-1}{2}}\left[\frac{F_{hkn}}{g(hkn)}\right].$$

The function $S'(x,y)$ was evaluated with the magnitudes of the F_{hkl}'s on an arbitrary scale, the signs being calculated from the atomic parameters obtained from the last $\varrho_z(x,y)$ map. The scale of $S'(x,y)$ was adjusted to make the average electron density of the bounded projection zero in regions where the heavy atoms do not appear in this projection. The parameters derived from this first bounded projection are given in column (3) of Table 2.

The bounded projection used here involves the difference of two separate series, the first a cosine series having as coefficients the F_{hk0} values and the second a sine series with the $(F_{hkl})/l$ values as coefficients. Distortion is introduced into the bounded projection if two series of unequal length are used, i.e. if the cosine and sine series are not terminated at the same value of $(\sin\theta)/\lambda$. A second source of distortion arises if the experimental threshold values of the observed F_{hkl} values are appreciably different for the $(hk0)$ and $(hk1)$ zones, since an inbalance in the number of terms of small magnitude in each of the two series results.

With these facts in mind, a second bounded projection was evaluated. The F_{hkl} values were put in on an absolute basis and no F_{hkl} term for which $(\sin\theta)/\lambda > 0{\cdot}7$ Å^{-1} was used. For each F_{hkl} observed to be absent, for reflections up to and including $(\sin\theta)/\lambda = 0{\cdot}7$ Å^{-1}, the experimentally determined threshold value was substituted. This second bounded projection (Fig. 3(*a*)) is relatively free from distortion and considerably improved in this respect over the first one. The $\varrho_z(x,y)$ map used in the preparation of this bounded projection is shown in Fig. 3(*b*).

Finally, a least-squares analysis of the x and y parameters of O_I, O_{II}, and O_{III} was carried out using unweighted coefficients, and based on the parameters of column (3), Table 2. The final parameters are given

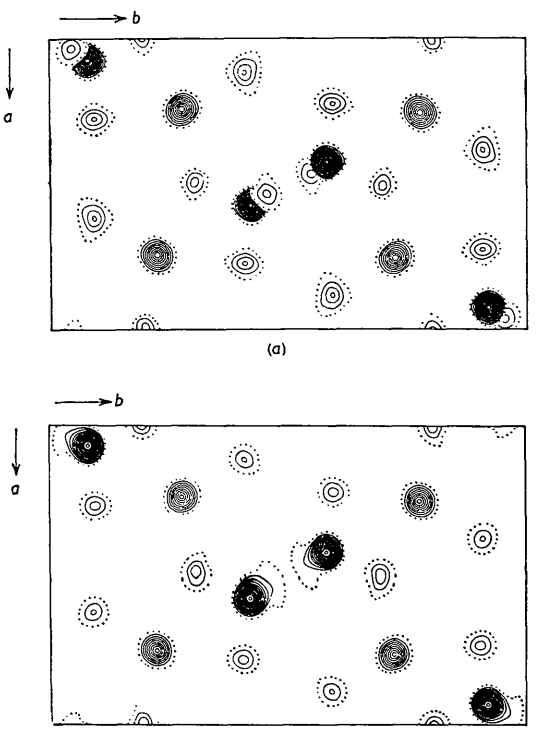

Fig. 3. (*a*) Projection on (001) of the superimposed electron-density maps taken between $z = 0$ and $z = \frac{1}{2}$ and between $z = \frac{1}{2}$ and $z = 1$ for $KVO_3.H_2O$. Contoured at intervals of 4 e.Å^{-2}, with the dotted contour equal to 4 e.Å^{-2}.
(*b*) Electron-density projection $\varrho_z(x,y)$ for $KVO_3.H_2O$. Contoured in same way as (*a*).

in column (4), Table 2. For O_I, O_{II}, and O_{III} these were obtained by applying the least-squares corrections. For the K, V, and H_2O parameters, the data of all of the electron-density projections were considered in arriving at the best choice. The standard errors associated with the oxygen atom parameters obtained from the least-squares analysis are very nearly the same for the three atoms; the averages are $\varepsilon_x = 0{\cdot}016$ Å and $\varepsilon_y = 0{\cdot}018$ Å. It was assumed that the limiting error in the V and K parameters was that of fixing the peak positions from the electron-density maps. Assuming this to be a maximum of 0·001 in cycles, the corresponding standard errors are $\varepsilon_x = 0{\cdot}004$ Å and $\varepsilon_y = 0{\cdot}007$ Å. The above errors lead to standard errors in the bond lengths of approximately $\pm 0{\cdot}02$ Å for V–O and K–O bonds and $\pm 0{\cdot}03$ Å for O–O bonds. The corresponding error in O–V–O bond angles is about $\pm 1°$. The precise positioning of the H_2O molecule was not considered to be of any real importance; the standard errors of its x and y parameters are of the order of 0·03 Å.

Throughout the course of the structure analysis, plots of R' versus $\sin\theta$, as suggested by Luzzati (1952), were found to be very helpful in deciding whether the structure was converging. Such a plot, based on the final parameters and compared with the corresponding theoretical curves of Luzzati, indicates a maximum mean error in bond length, $|\overline{\Delta r}| = 0{\cdot}04$ Å, entirely in agreement with the least-squares results.

Description and discussion of the structure

A pictorial view of the structure of $KVO_3.H_2O$ is given in Fig. 5, and a projected view in Fig. 4(*a*). It is seen

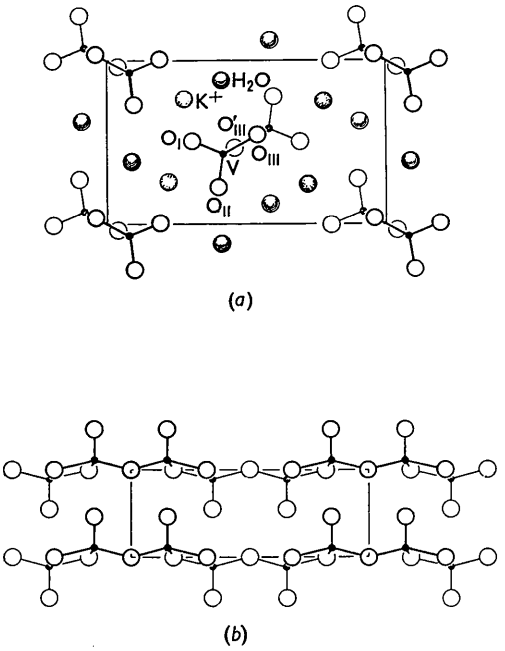

Fig. 4. (*a*) Structure of $KVO_3.H_2O$ projected on (001). (*b*) Structure of V_2O_5 projected on (001) (after Byström *et al.*, 1950).

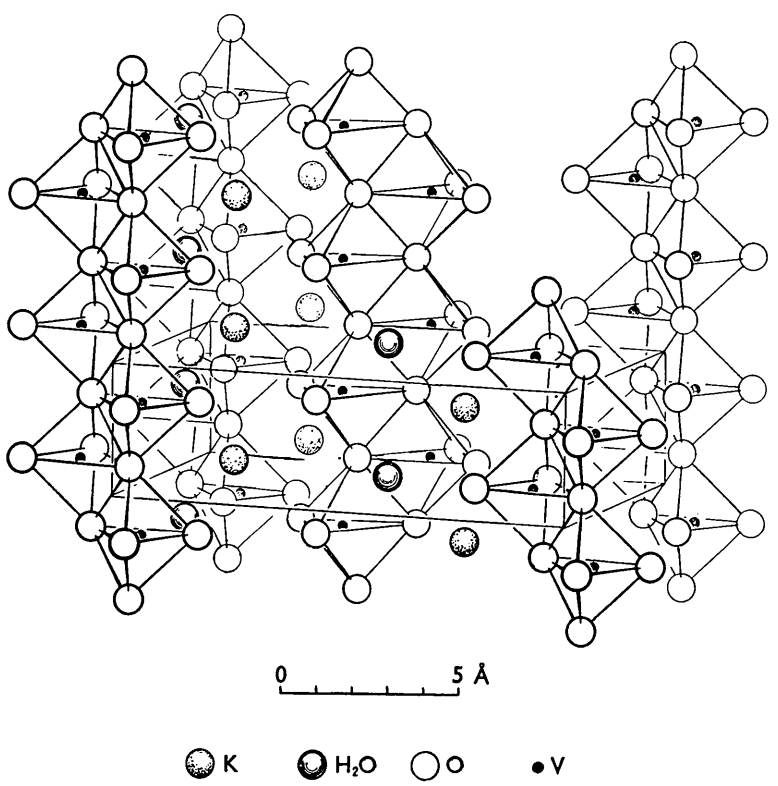

Fig. 5. Pictorial view of $KVO_3.H_2O$.

that each vanadium atom is linked to five oxygen atoms to form a distorted trigonal dipyramid. The trigonal dipyramidal polyhedra share edges to form continuous chains parallel to the *c* axis, accounting for the observed pronounced fibrous cleavage. The coordination of oxygen atoms around the vanadium atoms is shown in detail in Fig. 6; the corresponding

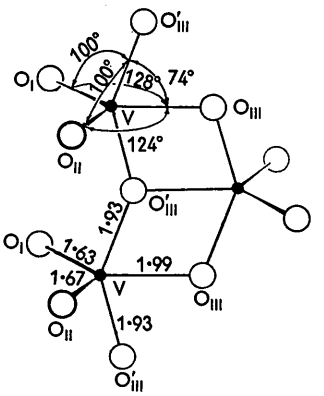

Fig. 6. Details of vanadium–oxygen coordination for $KVO_3.H_2O$.

V–O bond lengths and angles and other important bond lengths and angles in the structure are listed in Table 3. As shown in the projected view of Fig. 4(*a*),

Table 3. *Bond lengths and bond angles for* $KVO_3.H_2O$

Bond lengths (Å)		Bond angles (°)	
V–O_I	1·63	O_I–V–O_{II}	106
V–O_{II}	1·67	O_I–V–O_{III}	128
V–O'_{III}	1·93 (2)	O_{II}–V–O_{III}	124
V–O_{III}	1·99	O'_{III}–V–O'_{III}	147
(V–O bonds ±0·02 Å)		O_I–V–O'_{III}	100
		O_{II}–V–O'_{III}	100
		(all ±1°)	
O_I–O_{II}	2·64		
O_I–O'_{III}	2·73		
O_{II}–O'_{III}	2·75		
O_{III}–O'_{III}	2·34 (2)		
(O–O bonds ±0·03 Å)			
K–O_I	2·98 (2), 2·79 (2)		
K–O_{II}	3·10 (2)		
K–H_2O	2·79 (2)		
(K–O bonds ±0·02 Å; K–H_2O bonds ±0·04 Å)			
V–V	3·14±0·02		

O_I, O_{II}, and O_{III} lie at the vertices of a triangle containing the vanadium atom, which is displaced away from the center of the triangle toward the edge O_IO_{II}. The V–O bonds lying in the triangle are: V–O_I = 1·63, V–O_{II} = 1·67, V–O_{III} = 1·99 Å. The plane defined as that plane containing the vanadium atoms and parallel to the *c* axis also contains the O_{III} atoms. If the bond lengths V–O_I and V–O_{II} and the bond angles O_I–V–O_{III} and O_{II}–V–O_{III} were the same, respectively, this plane would then be a plane of symmetry. The lengths V–O_I and V–O_{II} were found to be 1·63±0·02 and 1·67±0·02 Å, respectively. A rough statistical calculation shows that there is high probability that the V–O_{II} bond is truly longer than the V–O_I bond. This conclusion is supported by the difference in bond angles found. It seems probable, therefore, that the chain does not conform exactly to a plane of symmetry. Detailed examination of the structure shows that the O_I–K and O_{II}–K lengths are different: K–O_I is 2·79±0·02 Å, and K–O_{II} is 3·10±0·02 Å. Thus it seems likely that the small departures from planar symmetry in the chain are due to packing effects, which result in overall lowering of the lattice energy. The O_{III}–O'_{III} distance of 2·34 Å is rather short and results from strong polarization of these atoms by the vanadium atoms. This postulated polarization is in agreement with the experimental observation that the atomic scattering curve for neutral vanadium gave better results than that for V^{+5}.

Fivefold coordination in crystals is rare. The only analogous situation seems to be that of V_2O_5 (Byström, Wilhelmi & Brotzen, 1950). In this compound there is a definitely similar distorted trigonal dipyramidal polyhedral chain linkage, as may be seen by comparing Fig. 4(*a*) and (*b*). The chains as found for $KVO_3.H_2O$ are further linked in V_2O_5 through oxygen atoms to form the more condensed system. The bond lengths of interest in the two compounds are compared in Table 4. For what has here been designated the V–O_I

Table 4. *Comparison of bond lengths for* $KVO_3.H_2O$ *and* V_2O_5

	$KVO_3.H_2O$	V_2O_5
V–O_I	1·63 Å	1·77±0·03 Å
V–O_{II}	1·67	1·54±0·06
V–O'_{III}	1·93	1·88±0·04
V–O_{III}	1·99	2·02±0·08
O_I–O_{II}	2·64	2·63
O_I–O'_{III}	2·73	2·70
O_{II}–O'_{III}	2·75	2·73
O_{III}–O'_{III}	2·34	2·39

bond, the length in V_2O_5 (1·77 Å) is significantly longer than that in $KVO_3.H_2O$ (1·63 Å). This difference is to be expected because in V_2O_5 it is the O_I atom that links the chains together to form sheets. The bond in V_2O_5 corresponding to the V–O_{II} bond of $KVO_3.H_2O$ is short, being only 1·54 Å in length, and must therefore be highly polarized. The differences in the configurations of the chains of the two compounds are such that, despite the much smaller V–O bond length in V_2O_5, the smallest O–O separations are nearly the same for the two compounds. The other bonds common to the two compounds have very nearly the same lengths. It is interesting that V_2O_5 is yellow red, whereas $KVO_3.H_2O$ is colorless. It is difficult to decide what differences in the bonding of the two compounds lead to this difference of absorption in the visible spectrum. It is hoped that the results of crystal-structure analysis of other vanadates being made in this and other laboratories will permit this question to be resolved later.

The K^+ of $KVO_3.H_2O$ is surrounded by six oxygen

Table 5. *Observed and calculated structure factors hk0 and hk1*

Values of F_c for *hk*0 are based on the atomic coordinates of column (4), Table 2; those for *hk*1 on the coordinates of column (3), Table 2.

hk0	F_o	F_c	hk0	F_o	F_c	hk0	F_o	F_c	hk0	F_o	F_c	hk0	F_o	F_c	hk0	F_o	F_c
000		304	210	48.4	-46.4	3,20,0		3.6	5,19,0	9.2	5.2	810	11.5	12.8	10,9,0	15.6	-18.5
200	15.4	13.5	220	69.6	69.0	3,21,0		5.8	5,20,0	11.5	13.2	820	29.2	-38.5	10,10,0		4.2
400	55.8	51.3	230	75.0	-78.7	3,22,0	17.4	16.4	5,21,0		4.6	830		1.7	10,11,0		- 7.9
600	63.7	-69.1	240	39.2	-33.5							840	20.2	23.3	10,12,0		7.1
800	6.1	7.8	250	47.4	-43.9	410	33.3	-29.8	610		- 5.3	850		7.0	10,13,0		9.6
10,0,0	7.2	-14.1	260		8.1	420	56.3	-56.5	620		0.1	860	11.3	10.3	10,14,0		- 7.1
12,0,0	16.6	17.9	270	20.5	18.9	430	72.2	-79.9	630		1.4	870		- 8.0	10,15,0		8.0
			280	46.6	-43.2	440	36.6	41.9	640		0.1	880	11.5	10.0			
020	10.2	9.8	290	43.3	38.5	450	39.7	-34.7	650	12.3	-16.2	890	15.9	-13.9	11,1,0	11.8	9.0
040	16.6	-12.0	2,10,0		- 3.7	460		4.1	660	50.9	57.5	8,10,0		5.1	11,2,0	14.3	12.3
060	105.2	-111.6	2,11,0	21.0	19.2	470	22.5	16.7	670	7.2	- 8.5	8,11,0		- 5.4	11,3,0		- 8.7
080	55.0	-46.7	2,12,0	22.3	21.6	480		2.2	680	7.7	6.3	8,12,0	17.7	-18.6	11,4,0	20.7	22.0
0,10,0	39.9	39.7	2,13,0	9.0	- 9.5	490	35.8	36.2	690		- 3.5	8,13,0		0.7	11,5,0		- 2.9
0,12,0	28.9	22.3	2,14,0		- 8.3	4,10,0		3.9	6,10,0	11.5	-14.5	8,14,0		0.8	11,6,0		- 9.5
0,14,0	25.9	26.2	2,15,0	25.3	-22.8	4,11,0	25.1	18.9	6,11,0		5.4	8,15,0	14.3	13.0	11,7,0	14.1	-12.6
0,16,0	20.7	-29.8	2,16,0	10.8	19.0	4,12,0	24.1	-27.7	6,12,0	22.8	-27.9	8,16,0		- 5.6	11,8,0		- 3.8
0,18,0	17.7	- 9.5	2,17,0	8.2	- 7.8	4,13,0	14.6	-13.6	6,13,0		9.7	8,17,0		6.3	11,9,0		8.4
0,20,0	8.4	-12.7	2,18,0	20.5	-26.0	4,14,0		4.2	6,14,0	20.7	-23.9	8,18,0	14.6	12.7	11,10,0	19.7	-23.3
0,22,0		18.1	2,19,0		6.5	4,15,0	20.5	-17.3	6,15,0		- 1.5				11,11,0		8.2
			2,20,0		6.5	4,16,0		- 8.3	6,16,0	18.2	23.7	910	18.7	-22.9	11,12,0		7.7
110	56.6	82.5	2,21,0	14.1	13.3	4,17,0	9.0	- 7.7	6,17,0		1.0	920	20.7	26.1	11,13,0		6.7
120	21.0	-22.3	2,22,0		- 3.4	4,18,0	9.0	17.3	6,18,0		0.6	930		- 2.0			
130	3.6	- 2.2				4,19,0		10.2	6,19,0		- 3.7	940	7.2	3.9	12,1,0		8.5
140	73.0	-73.8	310	56.8	55.6	4,20,0		- 2.4	6,20,0	16.1	15.0	950	18.2	18.9	12,2,0		-10.4
150	13.1	- 8.0	320	22.8	-45.6	4,21,0	15.6	10.4				960	12.0	12.9	12,3,0		0.4
160	41.2	41.7	330	18.7	-14.5				710	25.6	-25.5	970	16.6	19.6	12,4,0		4.3
170	53.2	-46.9	340	15.9	-11.6	510	23.8	-20.1	720	6.7	-12.4	980	24.1	-34.1	12,5,0	8.4	6.7
180	15.6	-18.2	350		- 4.5	520	41.0	-36.4	730	12.5	-13.5	990	7.7	- 6.1	12,6,0		-9.4
190	24.8	-19.5	360	53.0	-53.7	530	5.1	- 4.7	740	8.2	8.4	9,10,0		- 3.4	12,7,0		-4.5
1,10,0	40.2	45.6	370	35.6	-31.3	540	66.5	-73.4	750	33.0	35.6	9,11,0	8.2	- 4.6	12,8,0		-3.9
1,11,0	22.5	18.8	380	44.3	45.2	550	30.0	29.6	760	19.2	-25.7	9,12,0	7.7	- 9.6	12,9,0		-5.9
1,12,0	17.7	-24.8	390		0.3	560	21.8	22.1	770	18.7	17.7	9,13,0	9.0	-13.3	12,10,0		7.2
1,13,0	16.4	10.5	3,10,0	6.1	- 3.7	570	21.5	20.1	780	14.6	16.8	9,14,0	15.9	18.4	12,11,0		-2.7
1,14,0		3.7	3,11,0	12.5	10.2	580		- 2.1	790		10.4	9,15,0		7.0			
1,15,0	13.3	8.1	3,12,0	29.4	33.0	590		- 8.1	7,10,0	14.8	-19.5	9,16,0	10.0	9.6	13,1,0	9.5	8.7
1,16,0	14.1	-11.1	3,13,0		- 0.4	5,10,0	37.9	46.4	7,11,0	16.6	-16.6	9,17,0		7.2	13,2,0		7.5
1,17,0	14.3	-10.2	3,14,0	21.8	-22.4	5,11,0	12.0	- 8.8	7,12,0	10.2	16.0				13,3,0		-1.0
1,18,0		1.6	3,15,0		- 1.3	5,12,0	9.5	-16.7	7,13,0	23.0	-19.5	10,1,0	7.2	5.7	13,4,0		-2.8
1,19,0	16.1	-12.0	3,16,0	16.9	-10.0	5,13,0	22.0	-21.7	7,14,0		- 6.7	10,2,0	8.2	8.6	13,5,0		-11.2
1,20,0		8.9	3,17,0	8.2	- 5.6	5,14,0	7.2	- 4.5	7,15,0		- 3.4	10,3,0	22.3	24.4	13,6,0		7.7
1,21,0		1.9	3,18,0		- 4.5	5,15,0		3.7	7,16,0		6.8	10,4,0	8.2	-13.1	13,7,0		- 6.8
1,22,0		- 3.5	3,19,0		- 2.6	5,16,0	16.1	-13.8	7,17,0	13.3	10.4	10,5,0	8.2	3.8	13,8,0		-10.1
						5,17,0	9.0	7.5	7,18,0		3.0	10,6,0	8.2	8.9			
						5,18,0		3.5	7,19,0	16.1	10.8	10,7,0	8.2	- 8.6			
												10,8,0		- 3.0			

hk1	F_o	F_c	hk1	F_o	F_c	hk1	F_o	F_c	hk1	F_o	F_c	hk1	F_o	F_c	hk1	F_o	F_c	hk1	F_o	F_c
201	48.6	-51.8	1,22,1	12.4	10.7	3,16,1	8.1	-13.8	5,15,1	8.6	6.8	811	24.3	26.9	10,8,1	17.8	-12.7	13,7,1		6.1
401	55.1	-52.6	1,23,1		-12.5	3,17,1	17.8	11.6	5,16,1	8.6	8.2	821	15.1	16.2	10,9,1		2.6	13,8,1	13.5	15.4
601	21.6	20.4				3,18,1		- 0.4	5,17,1	16.2	16.6	831	6.5	- 1.0	10,10,1	14.0	10.3	13,9,1		- 8.2
801	17.3	12.7	211	58.9	-77.2	3,19,1	20.0	25.2	5,18,1		1.8	841	6.5	- 6.3	10,11,1		- 9.5	13,10,1		5.9
10,0,1	33.5	35.2	221	33.5	-29.2	3,20,1	9.7	8.1	5,19,1	14.6	12.4	851	23.8	23.3	10,12,1	17.3	13.0	13,11,1	13.0	15.2
12,0,1	9.2	2.8	231	46.4	46.1	3,25,1	18.4	-26.7				861	14.0	- 9.3	10,13,1		12.1			
14,0,1		7.1	241	35.6	33.3				611	14.6	-19.1	871	18.9	-19.0	10,14,1	13.5	11.1	14,1,1	14.6	-21.1
16,0,1	11.9	-14.8	251	27.0	-27.8				621		- 0.1	881	15.7	-14.6	10,15,1		- 5.2	14,2,1		- 6.5
			261	49.7	49.2				631	62.6	75.9	891	17.3	-14.0	10,16,1	8.6	- 7.9	14,3,1		- 6.1
011	*	-24.5	271	15.7	12.8	411	35.6	36.5	641		4.3	8,10,1	7.0	- 2.9	10,17,1		11.4	14,4,1		0.3
031	105.8	-132.4	281	20.0	21.3	421	23.2	-16.1	651	13.0	3.2	8,11,1	15.1	- 7.6	10,18,1	10.8	- 7.8	14,5,1	9.2	-15.1
051	14.0	6.8	291	33.5	35.4	431		6.3	661		- 3.6	8,12,1	16.2	8.8				14,6,1		- 4.0
071	36.7	32.3	2,10,1	18.4	-18.8	441	31.9	29.4	671	20.0	-17.1	8,13,1		- 6.5	11,1,1	25.9	24.6	14,7,1		5.1
091	75.6	78.2	2,11,1		- 2.0	451	43.2	40.8	681		- 0.4	8,14,1		4.3	11,2,1	12.4	-14.9	14,8,1		1.3
0,11,1	23.2	29.9	2,12,1	36.2	38.3	461	48.1	51.3	691	30.2	-26.9	8,15,1	23.8	29.5	11,3,1	7.6	- 8.8	14,9,1	10.8	15.0
0,13,1	33.5	-45.3	2,13,1		15.3	471	17.8	-17.7	6,10,1		0.7	8,21,1	10.8	-19.7	11,4,1	13.5	-14.4			
0,15,1	23.2	-19.6	2,14,1	18.4	-19.4	481	21.6	15.7	6,11,1	28.6	-30.7				11,5,1	10.8	- 5.6	15,1,1	9.2	-11.3
0,17,1	28.1	-43.2	2,15,1	25.4	-36.6	491		- 5.2	6,12,1	13.5	- 9.8				11,6,1		- 1.5	15,2,1	9.2	-10.8
0,19,1	19.4	29.4	2,16,1	8.1	7.3	4,10,1	30.8	-25.4	6,13,1	19.4	27.3	911	24.3	22.8	11,7,1	29.7	-34.8	15,3,1		- 7.1
0,21,1	16.2	7.9	2,17,1	8.6	- 3.2	4,11,1	11.9	- 4.6	6,14,1		- 6.3	921	17.3	15.3	11,8,1	8.1	4.0	15,4,1	10.8	-11.1
0,23,1	14.6	16.0	2,18,1	18.9	23.4	4,12,1	32.4	-38.4	6,15,1	18.4	9.8	931	10.8	12.5	11,9,1	9.7	11.4	15,5,1	13.0	18.3
			2,19,1		-13.2	4,13,1	9.2	-15.1	6,16,1		- 6.2	941	24.8	27.0	11,10,1	8.6	12.9	15,6,1		0.3
111	30.8	-37.1	2,20,1	13.5	14.1	4,14,1	21.6	-21.3	6,17,1	18.4	23.3	951	28.6	-34.8	11,11,1		4.6			
121	35.6	-36.4	2,21,1	15.7	18.4	4,15,1	20.5	28.0	6,18,1		6.7	961	15.1	-15.8	11,12,1		- 6.8			
131	34.0	34.4	2,22,1		- 2.0	4,16,1	14.6	13.3	6,19,1		-14.8	971	14.0	- 5.5	11,13,1	20.5	23.3	*Not registered.		
141	10.8	4.5	2,23,1		5.4	4,17,1		-15.3	6,20,1		8.0	981	16.7	-16.1						
151	7.0	- 8.5	2,24,1	13.0	-12.2	4,18,1	20.5	20.3	6,21,1	12.4	- 6.8	991	20.5	-22.4	12,1,1		5.1			
161	9.2	- 6.9				4,19,1	9.2	15.6				9,10,1	17.3	-20.3	12,2,1		7.9			
171	50.2	56.4	311	8.6	- 1.6	4,20,1	11.9	15.7	711	15.7	11.9	9,11,1	23.8	28.5	12,3,1	19.4	-21.4			
181	39.4	37.5	321	31.3	-31.0	4,24,1	10.8	- 9.5	721	28.1	23.6	9,12,1		3.9	12,4,1		- 6.5			
191	34.0	-41.4	331	29.2	-23.3				731	11.9	-12.1	9,13,1	9.2	3.9	12,5,1		- 0.7			
1,10,1	36.2	31.6	341	7.0	- 0.2	511	41.6	-38.2	741	34.0	30.6	9,14,1	18.9	18.8	12,6,1	9.2	- 4.5			
1,11,1		9.6	351	53.5	53.1	521	23.8	16.7	751	18.4	22.0	9,15,1	9.7	8.8	12,7,1		- 7.5			
1,12,1		- 1.5	361	8.6	2.7	531	24.3	25.1	761	5.9	1.5	9,16,1		12.0	12,8,1		- 7.7			
1,13,1	25.9	-31.3	371		-12.7	541	42.7	39.9	771	25.9	-26.9	9,17,1	10.3	-10.5	12,9,1	12.4	8.5			
1,14,1	17.8	-15.0	381	23.2	23.3	551	23.2	14.3	781	27.5	-27.1	9,18,1		0.7	12,10,1		1.2			
1,15,1		10.0	391	30.8	37.5	561	9.7	-11.6	791	11.9	17.8	9,19,1	13.0	-13.7	12,11,1		8.9			
1,16,1	27.5	-28.8	3,10,1	14.6	18.5	571	48.1	58.4	7,10,1	24.8	-20.9				12,12,1	12.4	9.3			
1,17,1	8.1	7.8	3,11,1	38.3	-46.6	581	15.7	-11.5	7,11,1	16.7	-23.2	10,1,1	16.7	-24.3						
1,18,1	8.6	- 9.9	3,12,1	14.0	-12.3	591	30.2	-35.1	7,12,1	14.6	-14.2	10,2,1	14.6	7.1	13,1,1		1.6			
1,19,1	9.2	1.5	3,13,1	18.4	-12.3	5,10,1	25.4	-19.9	7,13,1	7.6	6.9	10,3,1	14.6	15.2	13,2,1	17.3	-19.5			
1,20,1	13.0	9.6	3,14,1	7.6	- 6.7	5,11,1	15.7	-10.1	7,14,1	19.4	23.4	10,4,1	11.3	- 7.0	13,3,1		3.5			
1,21,1		9.2	3,15,1	16.7	-19.8	5,12,1	14.0	- 3.7	7,15,1		- 6.5	10,5,1	11.3	-13.9	13,4,1	9.2	-10.8			
						5,13,1	31.3	-42.5	7,16,1	22.7	19.0	10,6,1	23.2	-25.4	13,5,1	9.2	-12.9			
						5,14,1	16.7	15.0	7,21,1	13.0	- 2.9	10,7,1		- 2.2	13,6,1	9.2	-12.2			

atoms and two water molecules in roughly cubic coordination with the K–O bond lengths given in Table 3.

Comparisons of the observed and calculated structure factors for the zones (*hk*0) and (*hk*1) are listed in Table 5.

We are indebted to two colleagues of the U.S. Geological Survey: Richard F. Marvin, who furnished material for chemical analysis, and George B. Magin, Jr., who made the analysis. This work was completed as part of a program undertaken by the U.S. Geological Survey on behalf of the Division of Raw Materials of the Atomic Energy Commission.

References

Booth, A. D. (1948). *Fourier Technique in X-Ray Organic Structure Analysis*. Cambridge: University Press.

Buerger, M. J. (1951). *Acta Cryst.* **4**, 531.

Buerger, M. J. & Klein, G. E. (1945). *J. Appl. Phys.* **16**, 416.

Byström, A., Wilhelmi K.-A. & Brotzen, O. (1950). *Acta Chem. Scand.* **4**, 1119.

Christ, C. L., Clark, J. R. & Evans, H. T., Jr. (1953). *J. Chem. Phys.* **21**, 1114.

Cochran, W. (1948). *J. Sci. Instrum.* **25**, 253.

Ducret, L.-P. (1951). *Ann. Chim. Phys.* (12), **6**, 705.

Düllberg, P. (1903). *Z. phys. Chem.* **45**, 129.

Fock, A. (1889). *Z. Kristallogr.* **17**, 1.

International Tables for the Determination of Crystal Structures (1935). Berlin: Borntraeger.

Jander, G. & Jahr, K. F. (1933). *Z. anorg. Chem.* **212**, 1.

Luzzati, V. (1952). *Acta Cryst.* **5**, 802.

Norblad, J.-A. (1875). *Bull. Soc. Chim.* (2), **23**, 64.

Souchay, P. & Carpeni, G. (1946). *Bull. Soc. Chim.* (5), **13**, 160.